Doctoral Dissertation (Shinshu University)

Study for the development of a fabrication technology of the *Antheraea pernyi* fibroin

March 2019

ROZET SELENE

Interdisciplinary Graduate School of Science and Technology,

Shinshu University

Department of Bioscience and Textile Technology

CONTENTS

Chapter 1: General Introduction

Chapter 1. General Introduction.

1.1 Silk

Silk has been used as a fiber for textile for more than 8500 years [1 - 2]. Now, as a material, silk is recognized as the "Queen of fiber" due to its luster, softness, feel, and mechanical properties. Silk is made of two kinds of proteins: the fibroin and the sericin. Fibroin is the main protein to make silk fibers, and sericin plays the adhesive role in constructing cocoon by binding fibroin fibers together. The fibroin protein is biosynthesized at the posterior division of the silk gland in the silkworm, and the sericin is produced at the middle division surrounding the fibroin, therefore the cross section of cocoon fiber is observed as a core-shell structure (Fig. 1).

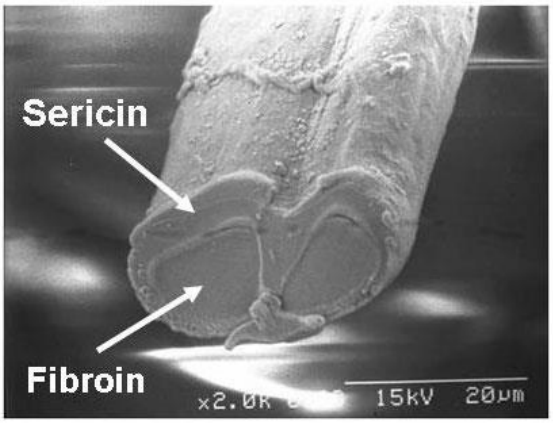

Fig. 1 SEM photograph of cross-section of a *Bombyx mori* cocoon fiber [3]

There are many kinds of silk producers among the insects. Spiders and Lepidoptera are the typical silk manufacturers. A study by Boulet-Audet et al. [4], presents the classification of Lepidoptera and spiders

determined by the structure of the silk fiber analyzed by infrared spectroscopy. As shown in Figure 2, five groups of silk species have been drawn when the Euclidean distance, the dissimilarity, was small enough. The five groups are the following:

- Group 1: *Caligula, Saturnia* and *Actias*,
- Group 2: *Argema*,
- Group 3: *Antheraea*,
- Group 4: *Attacus* and *Samia*,
- Group 5: *Bombyx*.

The group 5, *Bombyx mori* (*B. mori*), is known as the domestic silk and is manufactured by sericulture and reeling industries. Its main end-use is as a textile fiber. The other groups are known as wild silks and especially group 3, *Antheraea*, is probably the most famous in the wild silk groups. The *Antheraea* is gathered from fields mainly in Japan and China. It is also used as a textile fiber. But wild silks are expected as a new material to be utilized as a bio-resource because of its different properties from *B. mori* silk. We also think wild silk's possibilities as a new functional material are to be used especially in the medical field. We focused on *Antheraea pernyi* (*A. pernyi*) silk as wild silk in this study, because the cocoons are easily available from our university farm.

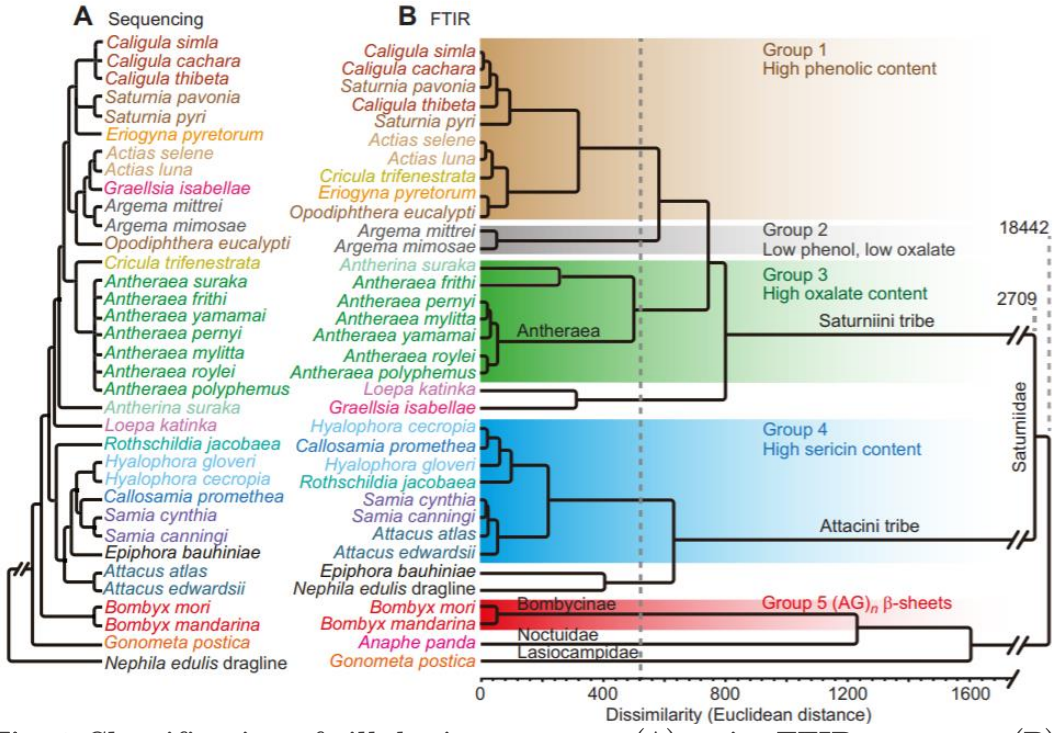

Fig. 2 Classification of silk by its sequence (A) or its FTIR structure (B), from Boulet-Audet et al. [4]

1.2 *A. pernyi* and *B. mori*

Many studies of *B. mori* fibes and fibroin concerning the structures (primary and higher ordered) [5 - 7], properties (mechanical, physicochemical, and physiological) [8 - 12], modifications (chemical and transgenetical) [13, 14] and applications (electrical, optical, and medical) [15 - 17] have been reported. Especially, the applications in medical are paid much attention recently. It comes from the fact that *B. mori* silk fibroin has been used as surgical suture for thousands of years [18 - 19] and the resulting biosafety. Recent studies revealed that *B. mori* fibroin has great properties such as biocompatibility and biodegradability [20 - 21] with cells and tissues. On the contrary, the number of studies

concerning with wild silks, like *A. pernyi,* are much fewer than *B. mori* fibroin [22].

From the past years, *A. pernyi* has been more and more studied and compared to the *B. mori*. Sezutsu et al. analyzed the dynamic rearrangement within the *A. pernyi* silk fibroin gene, proving the association of four types of repetitive units for its molecule [23]. The primary structure of the *A. pernyi* silk fibroin has been studied by Fu et al., putting in evidence the similarity of the wild silk with the spider silks and yet not as good but still better than the *B. mori* [24]. Also, Zhang et al. showed in their study that the *A. pernyi* could be a potential resource for artificially biospinning spider dragline silk thanks to its mechanical properties [25].

Guan et al. investigated the difference in the microstructure and mechanical properties between *B. mori* and *A. pernyi* cocoons composites. The cocoons share a similar fiber-network where the fibroin filaments are connected to each-other by sericin. However, they have different mechanical properties in their cocoons such as a higher density and lower porosity for the *A. pernyi* cocoons, along with a specific breaking energy three times greater than that of *B. mori* [26]. Du et al. also compared the interaction between fibroin and sericin proteins from *A. pernyi* and *B. mori* silk fibers. The results show the adhesion between sericin and fibroin in *A. pernyi* silks is stronger and more heterogeneous than that in *B. mori* silks, hence the difficulties to properly process the degumming process on *A. pernyi* fibers [27]. Want et al. and Zuo et al. investigated

the structure and properties of regenerated *A. pernyi* silk fibroin filaments, conducting a research on the molecular weight of the regenerated silk fibroin aqueous solution. The study also reported the regenerated *A. pernyi* silk fibroin has a crystalline structure similar to the native fiber with mainly a beta-sheet conformation but more alpha-helix and random coil conformation [28 - 29].

1.3 Medical applications of *A. pernyi* silk

Several studies where *A. pernyi* fibroin is used for medical applications have been reported. Since *A. pernyi* fibroin has RGD (Arg-Gly-Asp) sequence in the molecules [23], which is known as cell adhesion promoting sequence [30], *A. pernyi* fibroin materials are thought as a promising material in tissue engineering scaffold for cell compatibility. Three dimensional scaffolds are a very interesting tool for medical purposes, offering an effective scaffold for cell support and tissue regeneration. As a possible biomaterial, Zhao et al. checked the enzymatic degradation of *A. pernyi* silk fibroin 3D scaffolds and fibers [31]. Films and porous scaffolds have been used for in vitro and in vivo experiments to prove the good biocompatibility of the *A. pernyi* fibroin with cells. For example, the wild silk fibroin has been used for tendon scaffold [32] or spinal cord repairs [33]. Another study used the *A. pernyi* silk fibroin as powdered wound dressing on rats [34] or the blend P(LLA-CL) nanofibrous scaffold for peripheral nerve tissue engineering [35].

1.4 Fabrication of *A. pernyi* silk fibroin

The most important properties required to the materials used in medical field is safety to living body on not only materials themselves but also the fabrication processes. Once any toxicity regents including the solvents has been used in the process, it is difficult to ensure the safety of the fabricated materials. In the case of *B. mori* fibroin, the safety fabrication process based on water solvent as a safest solvent is established [10] including production of nanofiber mat by electrospinning using a fibroin aqueous solution as the spinning dope [36]. *A. pernyi* fibroin was also reported to make the aqueous solution for fabrication of materials with various forms like film.

Table 1 summarize some researches and their different method of preparation of the *A. pernyi* silk fibroin aqueous solution. Kweon et al. studied the dissolution and characterization of regenerated *A. pernyi* silk fibroin [37]. Tsukada et al. could prepare regenerated *A. pernyi* films by using lithium thiocyanate solvent and studied its stability with temperature changes [38]. Kweon et al. prepared regenerated *A. pernyi* silk fibroin films by using $Ca(NO_3)_2$ solution and studied the conformational changes after methanol or heat treatments [39 - 41] and the conformational change by ethanol treatment [42]. Lu et al. also investigated the preparation of water-insoluble *A. pernyi* silk fibroin films from the aqueous solution [43]. Liu et al. investigated the gelation of *A.*

pernyi silk fibroin and how it can be accelerated by shearing by inducing rapid physical intra- and inter-molecular cross-linking via ß-sheet formation [44]. Chemical crosslinking for *A. pernyi* regenerated silk fibroin compliant film was studied by Li et al. Mixing with at least 20 wt.% PEG-DE (Polyethylene glycol- Diglycidyl ether) in *A. pernyi* films could make an effective crosslinking reaction and retained an α-helix and random coil rich structure [45]. Blend films were also studied such as Poly-vinyl alcohol/fibroin blend films [46] or the fibroin/chitosan blend. Their structural and thermal characteristics were investigated by Kweon et al. who also investigated for drug delivery system [47, 48].

Table 1. Summary of the process conditions for preparation of *A. pernyi* fibroin Aqueous solution from previously reported papers

Solvent	Conditions	Dialysis conditions
10 M LiSCN	1 :10 (w/v) – 55°C – 2h	Water – 4d – 4°C [27]
Saturated LiSCN	1 :10 (w/v) – 50°C – 80 min	Water – 4d – RT [43]
9 M LiSCN	1 :10 (w/v) – 50°C – 1h	Water – 4d - RT [35]
9 M LiSCN	1 :10 (w/v) – 40°C – 1h	Water – 4d - RT [45]
7 M $Ca(NO_3)_2$	No data – 100°C – 3h	Water – 4d – RT [37]
10 M LiSCN	1 :10 (w/v) – 40°C – 1h	Water – 4d – RT [42]
$Ca(NO_3)_2 \cdot 4H_2O$	1 :10 (w/v) – 105°C – 5h	Water – 4d – RT [40, 44, 49]

According to these studies, the typical process to make the aqueous solution from *A. pernyi* cocoons is constructed by 1) degumming using $NaCO_3$ solution and sometimes washing the cocoon with $NaHSO_4$ for

removing calcium oxalate crystals on the cocoon, 2) dissolving in high concentration LiSCN solution or melted $Ca(NO_3)_2$, and 3) dialyzing against water for several days. As the first step of my study, we have traced the reported process to make the aqueous solution. However, we encountered difficulties to prepare *A. pernyi* fibroin aqueous solution with stability and reproducibility. The main problem was the gelation of the solution during the dialysis process. This easy gelation of *A. pernyi* fibroin may come from stronger interactions among the molecules because poly-(Ala) sequence in the primary structure like the spider dragline silk presents in its crystalline region. We have made great efforts to overcome the trouble, but all attempts could not be adapted to establish the process without gelation. It will be strictly required to prepare the aqueous solution with stability and reproducibility to manufacture *A. pernyi* fibroin materials used in medical field.

1.5 Objective

The objective of my study is the development of a new fabrication technology of *A. pernyi* fibroin from the aqueous solution and aiming at its utilization as a medical material such as a tissue engineering scaffold.

The first part of the study is a basic research on the improvement of the process to make an aqueous solution with stability and reproducibility. Each process, which includes degumming, dissolving, and dialyzing steps,

are reconfirmed by examining every condition possible. Then, the *A. pernyi* fibroin in the aqueous solution is characterized.

The second part of the study is the fabrication of *A. pernyi* fibroin coating films using the aqueous solution. The structure, surface morphology and physicochemical properties, and cell compatibility are determined and compared with other previous reports and *B. mori* fibroin films.

References

1) V. B. Khyade: Silk route: The unesco world heritage.

2) Y. Gong, L. Li, D. Gong, H. Yin, and J. Zhang (2016): Biomolecular evidence of silk from 8,500 years ago, PloS one, **11** (12), e0168042.

3) F. Ashan (2015): Silk functionalization: Developing the next generation of high-performance fibers [Article].
Retrieved from: http://parts.igem.org/Part:BBa_K1763444

4) M. Boulet-Audet, F. Vollrath, and C. Holland (2015): Identification and classification of silks using infrared spectroscopy, J Exp Biol, 128-306.

5) M. M. R. Khan, H. Morikawa, Y. Gotoh, M. Miura, Z. Ming, Y. Sato, and M. Iwasa (2008): Structural characteristics and properties of *Bombyx mori* silk fiber obtained by different artificial forcibly silking speeds, Int J Biol Macromol, **42** (3), 264–270.

6) Y. Cao and B. Wang (2009): Biodegradation of silk biomaterials, Int J Mol Sci, **10** (4), 1514–1524.

7) A. Ude, R. Eshkoor, R. Zulkifili, A. Ariffin, A. Dzuraidah, and C. Azhari (2014): *Bombyx mori* silk fibre and its composite: a review of contemporary developments, Mater Design, **57**, 298–305.

8) T. Arai, G. Freddi, R. Innocenti, and M. Tsukada (2004): Biodegradation of *Bombyx mori* silk fibroin fibers and films, J Appl Polym Sci, **91** (4), 2383–2390.

9) N. Minoura, M. Tsukada, and M. Nagura (1990): Physicochemical properties of silk fibroin membrane as a biomaterial, Biomaterials, **11** (6), 430–434.

10) D. N. Rockwood, R. C. Preda, T. Y¨ucel, X. Wang, M. L. Lovett, and D. L. Kaplan (2011): Materials fabrication from *Bombyx mori* silk fibroin, Natureprotocols, **6** (10), 1612.

11) Y. Yang, Z. Shao, X. Chen, and P. Zhou (2004): Optical spectroscopy to investigate the structure of regenerated *Bombyx mori* silk fibroin in solution, Biomacromolecules, **5** (3), 773–779.

12) M. Mondal (2007): The silk proteins, sericin and fibroin in silkworm, *Bombyx mori* linn.,-a review, Caspian J. Environm. Sci, **5** (2), 63–76.

13) H. Wen, X. Lan, Y. Zhang, T. Zhao, Y. Wang, Z. Kajiura, and M. Nakagaki (2010): Transgenic silkworms (*Bombyx mori*) produce recombinant spider dragline silk in cocoons, Mol Biol Rep, **37** (4), 1815–1821.

14) M. Tomita, H. Munetsuna, T. Sato, T. Adachi, R. Hino, M. Hayashi, K. Shimizu, N. Nakamura, T. Tamura, and K. Yoshizato (2003): Transgenic silkworms produce recombinant human type iii procollagen in cocoons, Nat Biotechnol, **21** (1), 52.

15) E. S. Gil, B. Panilaitis, E. Bellas, and D. L. Kaplan (2013): Functionalized silk biomaterials for wound healing, Adv Healthc Mater, **2** (1), 206– 217.

16) B.-M. Min, L. Jeong, Y. S. Nam, J.-M. Kim, J. Y. Kim, and W. H. Park (2004): Formation of silk fibroin matrices with different texture and its cellular response to normal human keratinocytes, Int J Biol Macromol, **34** (5), 223–230.

17) M. Kang and H.-J. Jin (2007): Electrically conducting electrospun silk membranes fabricated by adsorption of carbon nanotubes, Colloid Polym Sci, **285** (10), 1163–1167.

18) R. L. Moy, A. Lee, and A. Zalka (1991): Commonly used suture materials in skin surgery. Am Fam Physician, **44** (6), 2123–2128.

19) G. H. Altman, F. Diaz, C. Jakuba, T. Calabro, R. L. Horan, J. Chen, H. Lu, J. Richmond, and D. L. Kaplan (2003): Silk-based biomaterials, Biomaterials, **24** (3), 401–416.

20) A. S. Lammel, X. Hu, S.-H. Park, D. L. Kaplan, and T. R. Scheibel (2010): Controlling silk fibroin particle features for drug delivery, Biomaterials, **31** (16), 4583–4591.

21) M. Li, M. Ogiso, and N. Minoura (2003): Enzymatic degradation behavior of porous silk fibroin sheets, Biomaterials, **24** (2), 357–365.

22) S. Sahoo, S. L. Toh, and J. C. Goh (2010): A BFGF releasing silk/PLGA-based biohybrid scaffold for ligament/tendon tissue engineering using mesenchymal progenitor cells, Biomaterials, **31** (11), 2990–2998.

23) H. Sezutsu and K. Yukuhiro (2000): Dynamic rearrangement within the *Antheraea pernyi* silk fibroin gene is associated with four types of repetitive units, J Mol Evol, **51** (4), 329–338.

24) C. Fu, D. Porter, X. Chen, F. Vollrath, and Z. Shao (2011): Understanding the mechanical properties of *Antheraea pernyi* silk from primary structure to condensed structure of the protein, Adv Funct Mater, **21** (4), 729–737.

25) Y. Zhang, H. Yang, H. Shao, and X. Hu (2010): *Antheraea pernyi* silk fiber: a potential resource for artificially biospinning spider dragline silk, Biomed Res Int, **2010**, 683962.

26) J. Guan, W. Zhu, B. Liu, K. Yang, F. Vollrath, and J. Xu (2017): Comparing the microstructure and mechanical properties of *Bombyx mori* and *Antheraea pernyi* cocoon composites, Acta Biomater, **47**, 60–70.

27) S. Du, J. Zhang, W. T. Zhou, Q. X. Li, G. W. Greene, H. J. Zhu, J. L. Li, and X. G. Wang (2016): Interactions between fibroin and sericin proteins from *Antheraea pernyi* and *Bombyx mori* silk fibers, J Colloid Interf Sci, **478**, 316–323.

28) B. Zuo, L. Liu, and F. Zhang (2009): Structure and properties of regenerated *Antheraea pernyi* silk fibroin filaments," J Appl Polym Sci, **113** (4), 2160–2165.

29) Y. Wang, J. Guan, N. Hawkins, D. Porter, and Z. Shao (2014): Understanding the variability of properties in *Antheraea pernyi* silk fibres, Soft matter, **10** (33), 6321–6331.

30) E. Ruoslahti and M. D. Pierschbacher (1987): New perspectives in cell adhesion: RGD and integrins, Science, **238** (4826), 491–497.

31) C. Zhao, X. Wu, Q. Zhang, S. Yan, and M. Li (2011): Enzymatic degradation of *Antheraea pernyi* silk fibroin 3D scaffolds and fibers, Int J Biol Macromol, **48** (2), 249–255.

32) Q. Fang, D. Chen, Z. Yang, and M. Li (2009): In vitro and in vivo research on using *Antheraea pernyi* silk fibroin as tissue engineering tendon scaffolds, Mater Sci Eng: C, **29** (5), 1527–1534.

33) A. Varone, D. Knight, S. Lesage, F. Vollrath, A. Rajnicek, and W. Huang (2017): The potential of *Antheraea pernyi* silk for spinal cord repair, Sci Rep-Uk, **7** (1), 13790.

34) M.-K. Kim, K.-Y. Yoo, K.-J. Kwon, S.-G. Kim, Y.- W. Park, K.-G. Lee, Y.-Y. Jo, and H.-Y. Kweon (2014): Powdered wound dressing materials made from wild silkworm *Antheraea pernyi* silk fibroin on full-skin thickness burn wounds on rats, Maxillofac Plast Reconstr Surg, **36** (3), 111.

35) J. Wang, B. Sun, M. A. Bhutto, T. Zhu, K. Yu, J. Bao, Y. Morsi, H. El-Hamshary, M. El-Newehy, and X. Mo (2017): Fabrication and characterization of *Antheraea pernyi* silk fibroin-blended P(LLA-CL) nanofibrous scaffolds for peripheral nerve tissue engineering, Front Mater Sci, **11** (1), 22–32.

36) Y. Kishimoto, H. Morikawa, S. Yamanaka, and Y. Tamada (2017): Electrospinning of silk fibroin from all aqueous solution at low concentration, Mater Sci Eng: C, **73**, 498–506.

37) H. Kweon and Y. H. Park (2001): Dissolution and characterization of regenerated *Antheraea pernyi* silk fibroin, J Appl Polym Sci, **82** (3), 750–758.

38) M. Tsukada, G. Freddi, Y. Gotoh, and N. Kasai (1994): Physical and chemical properties of tussah silk fibroin films, J. Polym. Sci. Polym. Phys, **32** (8), 1407–1412.

39) H. Y. Kweon and Y. H. Park (1999): Structural and conformational changes of regenerated *Antheraea pernyi* silk fibroin films treated with methanol solution, J Appl Polym Sci, **73** (14), 2887–2894.

40) H. Kweon, S. O. Woo, and Y. H. Park (2001): Effect of heat treatment on the structural and conformational changes of regenerated *Antheraea pernyi* silk fibroin films, J Appl Polym Sci, **81** (9), 2271–2276.

41) H. Kweon, I. Um, and Y. Park (2000): Thermal behavior of regenerated *Antheraea pernyi* silk fibroin film treated with aqueous methanol, Polymer, **41** (20), 7361–7367.

42) M. Li, W. Tao, S. Kuga, and Y. Nishiyama (2003): Controlling molecular conformation of regenerated wild silk fibroin by aqueous ethanol treatment, Polym Advan Technol, **14** (10), 694–698.

43) S. Z. Lu, L. Mao, Y. Liu, S. Sun, and G. J. Li (2012): Preparation of water-insoluble *Antheraea pernyi* silk fibroin films, Adv Mat Res, **569**, 311–315.

44) Y. Liu, S. Xiong, R. You, and M. Li (2013): Gelation of *Antheraea pernyi* silk fibroin accelerated by shearing, Materials Sciences and Applications, **4** (6), 365.

45) M. Li, W. Tao, S. Lu, and S. Kuga (2003): Compliant film of regenerated *Antheraea pernyi* silk fibroin by chemical crosslinking, Int J Biol Macromol, **32** (3-5), 159–163.

46) T. Tanaka, T. Tanigami, and K. Yamaura (1998): Phase separation structure in poly (vinyl alcohol)/silk fibroin blend films, Polym Int, **45** (2), 175–184.

47) R. Rujiravanit, S. Kruaykitanon, A. M. Jamieson, and S. Tokura (2003): Preparation of crosslinked chitosan/silk fibroin blend films for drug delivery system, Macromol Biosci, **3** (10), 604–611.

48) H. Kweon, H. C. Ha, I. C. Um, and Y. H. Park (2001): Physical properties of silk fibroin/chitosan blend films, J Appl Polym Sci, **80** (7), 928–934.

49) S. Yan, C. Zhao, X. Wu, Q. Zhang, and M. Li (2010): Gelation behavior of *Antheraea pernyi* silk fibroin, Sci China Chem, **53** (3), 535–541.

Chapter 2: Improvement process for preparation of *Antheraea pernyi* fibroin aqueous solution

1. Introduction

The *Antheraea pernyi* silk, which is a kind of wild silks, has recently gathered attention as a biomaterial for cell culture substrate, gene delivery carrier, and cell scaffold in tissue regeneration [1 - 5]. *A. pernyi* silk fibroin molecules have an Arg-Gly-Asp (RGD) tripeptide sequence [6] which can bind to integrin receptors in cell membrane and facilitate adhesion of many kinds of cells [7].

A. pernyi degummed fiber filaments were reported for the development of a nerve guidance for spinal cord repair [8], while regenerated *A. pernyi* fibroin materials like film, sponge, and gel were fabricated for wide variety of applications as biomaterial from the *A. pernyi* fibroin aqueous solution [1, 9]. Several procedures were reported to prepare the aqueous solution. *A. pernyi* fibroin liquid was collected from the posterior silk gland of a mature larva and dispersed in deionized water [10, 11]. Pure *A. pernyi* aqueous solution can be obtained by this procedure, but the process requires a skilled handwork and the amount of fibroin is too little to fabricate various kinds of materials. Degummed cocoons are a useful source for preparation of *A. pernyi* fibroin. High concentrated LiSCN solution and melted $Ca(NO_3)_2$ are typical solvents for dissolving the *A. pernyi* fibroin fibers according to the literature [12]. The reported process explains that the degummed *A. pernyi* fibers are dissolved in the above-mentioned solvents while heating and stirring, then the solution is dialyzed against water for several days. However, when making the aqueous solution under the same published conditions, we often experienced gelation and aggregation of *A. pernyi* fibroin. It is inferred that since the *A. pernyi* fibroin is easy to aggregate and self-assemble due to the strong

intermolecular interactions through the hydrogen bonding in β-sheet structure consisted by the poly-Ala sequences [13], a subtle difference in the environment during the preparation process will affect the molecular aggregation in the solution. Stable and reproducible production system is very important for the industrial applications of *A. pernyi* fibroin. In this study, we reconsidered the whole process to make *A. pernyi* fibroin aqueous solution from the cocoons and reported an improved process to produce the aqueous solution with stability and reproducibility.

2. Materials and Methods

2.1 *A. pernyi* cocoons

A. pernyi silkworms were bred at the farm of Shinshu University, Ueda, and the collected and stored cocoons were kindly supplied by Prof. Z. Kajiura, Shinshu University.

2.2 Degumming

A. pernyi cocoons were cut in small pieces and degummed with 2.5 w/v% Na_2CO_3 solution at 95-98 ℃ for 30 mins, and then washed three times with hot water and dried at 50 ℃ overnight. The degumming process was repeated three times. The degumming ratio at each time was determined by the equation as follows:

Degumming ratio(%) = (W0 – W1)/W0 x 100

W0 and W1 are the weight of the cocoons before and after degumming, respectively.

In order to examine washing effects of the cocoons, before degumming process, the cocoons were washed with water for 30 mins at room temperature or with 0.05% of $NaHSO_4$ solution for 5 mins at 95 ℃.

2.3 Dissolving and dialysis

0.25 g of the degummed fibers were dissolved in 2.5 mL of lithium thiocyanate (LiSCN, Wako pure chemical Co. Ltd., Japan) at 10 to 16 M concentrations. The dissolving process was performed at 45 ℃ for 1 hour with shaking in water bath, and the solubility was judged by the appearance of the solutions considering the existence of visible fibers in the solution. The dissolved *A. pernyi* fibroin solutions were poured into a cellulose dialysis tube (MWCO 6000-8000, Spectrapore, Tokyo, Japan) and followed by dialysis process. The dialysis process was conducted using the bath ratio of the dialysis solution to fibroin solution of 150 at room temperature. The changing of the dialysis solution and duration of dialysis was changed according to the designed protocol of each experiment. The dialysis was confirmed by measurement of the conductivity of the dialysis solutions using conductivity meter (Laqua, F-74BW, Horiba Co. Ltd., Tokyo, Japan). The concentration of the aqueous solution was determined by weighting the remaining solid after drying the solution.

2.4 Analytical methods

Surface morphology of native and degummed fibers was observed by Scanning Electron Micrograph (SEM, JEOL, JSM-6010LA, 10 kV, Tokyo, Japan) after Au coating. Particle distribution in the aqueous solution was

measured by dynamic light scattering (DLS, Malvern Instruments Zen3600, Malvern, UK) and the amount of Ca^{2+} ions were determined by inductivity coupled plasma optical emission spectrometer (ICP-OES, Hitachi, SPS3100, Tokyo, Japan).

3. Results and Discussion

3.1 Degumming and dissolving

For degumming of *A. pernyi* cocoons, we performed the pretreatment with $NaHSO_4$ solution because calcium oxalate crystals are existing of the cocoons [14 - 16]. We thought the crystals might be influencing the degumming and solubilizing process to make *A. pernyi* aqueous solution. Figure 1 shows the SEM images of the external and internal surface of *A. pernyi* cocoon before and after pretreatment with water and $NaHSO_4$. The $NaHSO_4$ solution washing was effective to remove the crystals from *A. pernyi* cocoons as shown in Figure 1 (c). Indeed, the oxalic acid is a weak acid when in solution and the oxalate ions from the calcium oxalate crystals prefer binding to become oxalic acids. The oxalate ions are therefore supplied by the calcium oxalate present on the fibres and because of the acidic condition of the solution, will turn to oxalic acid.

Figure 2 shows the weight change of *A. pernyi* cocoons by the $NaHSO_4$ washing and degumming. The amount of the crystals was estimated at approximately 12 wt % of the cocoon weight [17]. Degumming was

performed three times according to the report by Tao et al. [10]. In our study, the degumming ratio was increased slightly at each degumming process. The final degumming ratio after 3 times degumming, are summarized in the table inserted in Figure 2. The degumming ratio of the native cocoon without prewashing was calculated at 21.9 %, while 14.1 % and 16.6 % of the degumming ratio from the $NaHSO_4$ and water pretreatment cocoons were evaluated, respectively. This difference is clearly explained by the crystals and debris existing on the native cocoons. And since $NaHSO_4$ solution is better solvent for dissolving of the oxalate crystal than water, the degumming ratio of the $NaHSO_4$ pretreatment cocoon will decrease comparing with water pretreatment cocoon.

It has been reported to dissolve *A. pernyi* fibroin with fluorinated organic solvents like hexafluoro isopropanol [18], strong acids like formic acid, high concentrated salt solutions like LiSCN and melted $CaNO_3$ [12]. We used LiSCN solution for dissolving *A. pernyi* fibroin because of the safety and handling. Although 10 M LiSCN solution was tried to dissolve our *A. pernyi* fibroin at 40 ℃ according to the report by Kweon et al. [12], it was hard to dissolve completely even if the solution was kept at high temperature. Therefore, we examined the conditions for dissolving our *A. pernyi* fibroin, and the results are summarized in Table 1. Our *A. pernyi* fibroin could not dissolve completely with less than 12 M LiSCN solution even if the concentration was low and the temperature was high, but a higher concentration than 12 M LiSCN solution could work to dissolve

our *A. pernyi* fibroin as shown in Figure 3. And no influence of the pretreatment process on solubility of *A. pernyi* fibroin was observed.

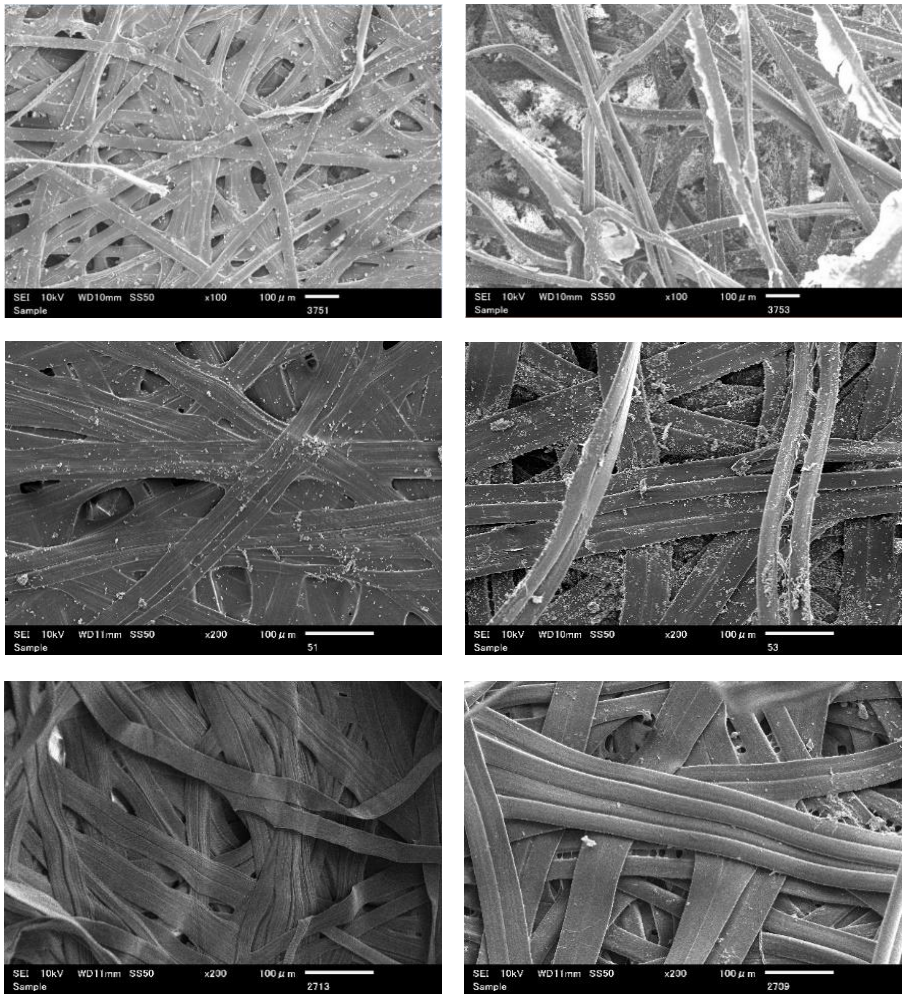

Fig. 1. SEM images of pieces of cocoons before the degumming process. On the left, the inside part of the cocoons and on the right, the external part of the cocoon. (a) Native cocoon without pretreatment; (b) after water pretreatment; (c) after $NaHSO_4$ pretreatment.

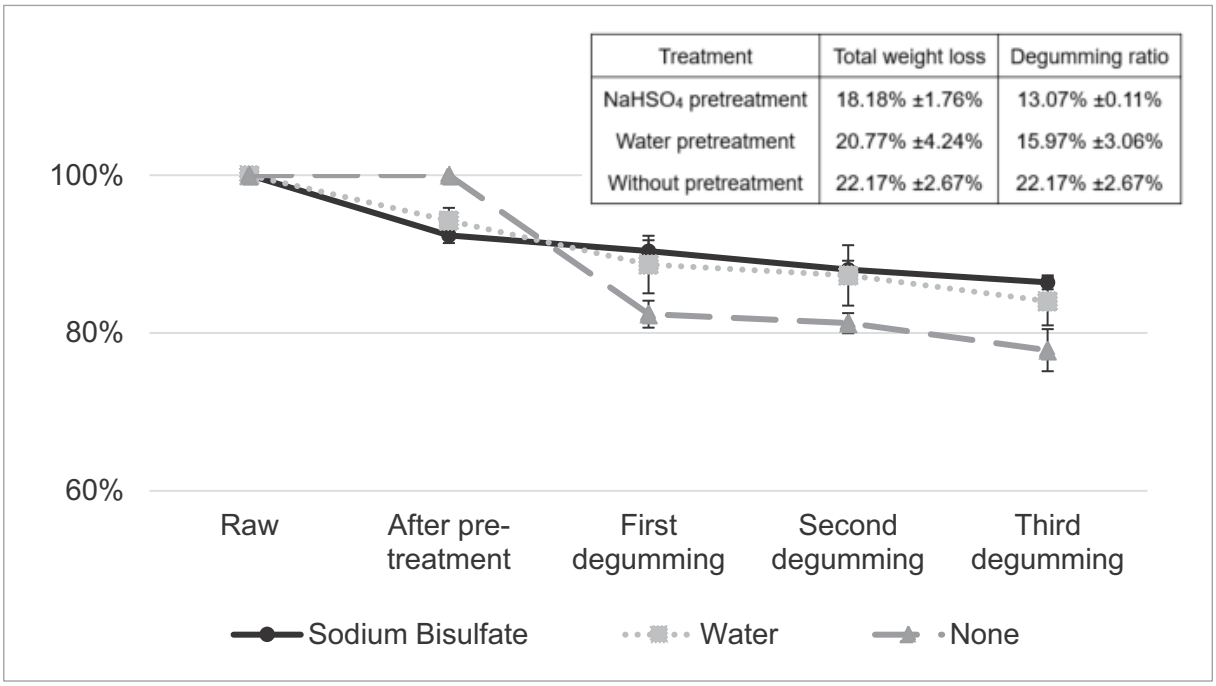

Fig. 2. Weight loss through pretreatment and degumming processes of *A. pernyi* fibers and degumming ratio (inserted table). N=4 for without treatment and N=3 for $NAHSO_4$ and error bars represent their standard deviation. N=2 for water pretreatment and the error bars represent the differences of the two data.

Table 1. Conditions of dissolving *A. pernyi* fibers at 3, 5 and 10% concentration and dissolution results. (*) ○ : No fibers were remained apparently, △ : Small amount of fibers were presented, ×: Original fibers were remained.

LiSCN concentration	Temperature	Time	Dissolution *
3, 5 and 10% in 10 M	45°C	1h	X
	95°C	1h	X
3, 5 and 10% in 12 M	45°C	1h	X
	95°C	1h	Δ
3, 5 and 10% > 12M	45°C	30 mins	O

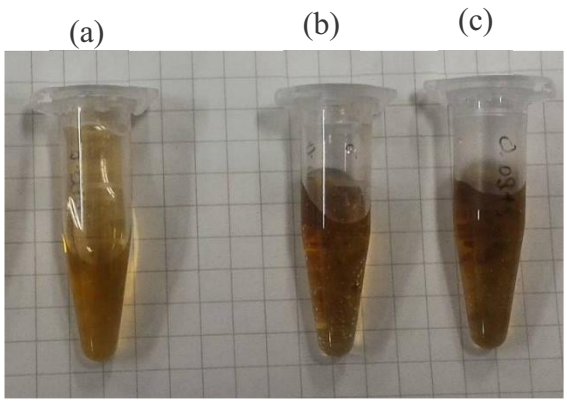

Fig. 3. Appearance of the *A. pernyi* fibroin solutions dissolved with 15 M LiSCN from degummed fibers (a) without pretreatment, (b) with water pretreatment, and (c) with $NaHSO_4$ pretreatment.

3.2 Dialysis process

In order to prepare *A. pernyi* aqueous solution, a dialysis process against water is required. The *A. pernyi* fibroin LiSCN solution at 12 M concentration as prepared above was dialyzed against water, but the solutions have turned to gel quickly in dialysis tube. We attempted to increase the concentration of LiSCN for preventing gelation during dialysis by the improvement of dissolving state. More than 15 M LiSCN was effective to prolong the gelation time up to 3 days, but finally the solution turned to gel during dialysis. We attempted to shorten the dialysis duration by decreasing the interval time of changing the dialysis solution from every 12 hr to 1 hr, but the gelation has occurred at the first dialysis stage. Yan et al. reported calcium and potassium ion help to delay the gelation of *A. pernyi* solution [13]. We added $CaCl_2$ in the dialysis solution at the first and second time of the dialysis. The *A. pernyi*

solutions dissolved with less than 14 M LiSCN were turned to gel quickly as same situation without $CaCl_2$, but the *A. pernyi* solutions prepared with more than 15 M LiSCN could be delayed the gelation by addition of $CaCl_2$ in the dialysis solution at the first and second time, but the gelation occurred at the end of dialysis (3 days) in the dialysis tube or during storage in refrigerator soon after dialysis. We found the gelation was prevented for more than 7 days by shortening the dialysis duration in the case of the *A. pernyi* solution dissolved with more than 15 M LiSCN. In order to confirm the dialysis process, we measured the change of the conductivity of the dialysis solution every 2 minutes during the dialysis. As shown in Figure 4, the conductivity of the dialysis solution both with and without $CaCl_2$ increased during the first process due to the excluded LiSCN and the conductivity reached to a constant value within 2 hours after starting the dialysis. And, after 3 times of changing the dialysis solution, the conductivity of the solution reached to the same level of pure water. This result indicates that our dialysis process which consists to change the dialysis solution every 1 hr and repeat the changing by more than 3 times, work well for preparation of *A. pernyi* aqueous solution. The dialysis process conditions and the gelation results are summarized in Table 2.

The *A. pernyi* solution dissolved with less than 14 M LiSCN has turned to gel quickly even with the addition of $CaCl_2$ in the dialysis solution and the decrease of the dialysis duration within every 1 hr. On the other hand, no gelation of the *A. pernyi* solution dissolved with more

than 15 M LiSCN occurred by addition of $CaCl_2$ and shortening the dialysis duration. We infer the undissolved *A. pernyi* particles remained in the solution under low concentration of LiSCN and the particles might be the trigger of the gelation during dialysis. In order to determine the existence of the particles in the *LiSCN* solution, DLS was performed. Figure 5 shows the results and indicates the diameter of 2 – 10 nm range particles were inside all *A. pernyi* solutions. This result will indicate the gelation trigger is not the undissolved *A. pernyi* particle but might be the self-assemble or self-coagulate molecules in the solution. Lower concentration of LiSCN will cause more self-assemble molecular complexes, and the molecular complexes will be the trigger of the gelation. Another possibility of the gelation trigger is the slightly acidic solution as shown by the pH measurement shown in Figure 4. The isoelectric point (pI) of the *A. pernyi* is reported around 4.3 [13], and the pH of the dialysis solution presented around pH 5.5 which is close to pI of *A. pernyi*. Therefore *A. pernyi* might has the tendency to aggregate in the dialysis conditions. Changing the pH of the dialysate to compensate has been tried (with pH 4, 7 and 9). However, results did not show improvements as the solution turned to gel each time. However, *A. pernyi* solution prepared by our $CaCl_2$ process did not turn to gel even in this slightly acidic dialysis conditions. Adjustment of pH of the dialysis solution might be a useful method to inhibit the gelation of *A. pernyi*, but the additional process to adjust the pH of the dialysis solution will be required. Our $CaCl_2$ process can use pure water as the dialysis solution.

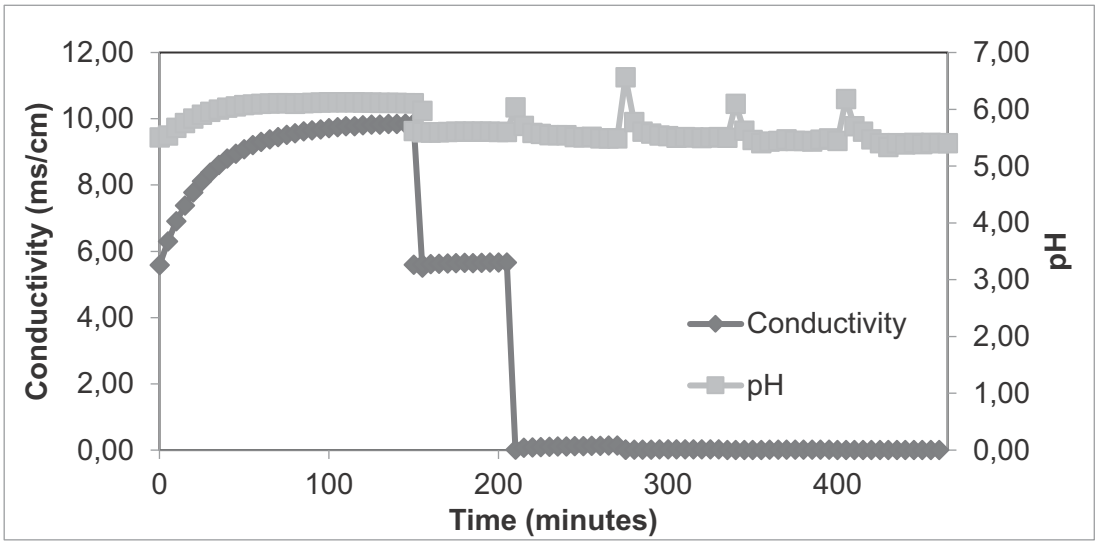

Fig. 4. Conductivity and pH of dialysis solution during dialysis against 25 mM $CaCl_2$ for *A. pernyi* solution dissolved in 14.5 M LiSCN

Table 2. Dialysis process conditions and the gelation results. C# indicates the times of the change of dialysis solution. C1 means the first time of dialysis solution change. - : not experimented

LiSCN concentration for dissolving	C1 -> C6 Water Change every 12h	C1 -> C6 Water Change every 8h	C1 -> C6 Water Change every 1h	C1 -> C2 25mM $CaCl_2$ C3 -> C6 water Change every 12h	C1 -> C2 25mM $CaCl_2$ C3 -> C6 water Change every 8h	C1 -> C2 25mM $CaCl_2$ C3 -> C6 water Change every 1h
12 M	Instant	Instant	Instant	Instant	Instant	~1h
13 M	Instant	Instant	Instant	~1h	~1h	~1h
14 M	Instant	Instant	Instant	~1h	~1h	~1h
14.5 M	-	3h	-	-	-	6h~
15 M	1h	1h	-	3 days	3 days	>3 months
16 M	1h	1h	-	3 days	3 days	>3months

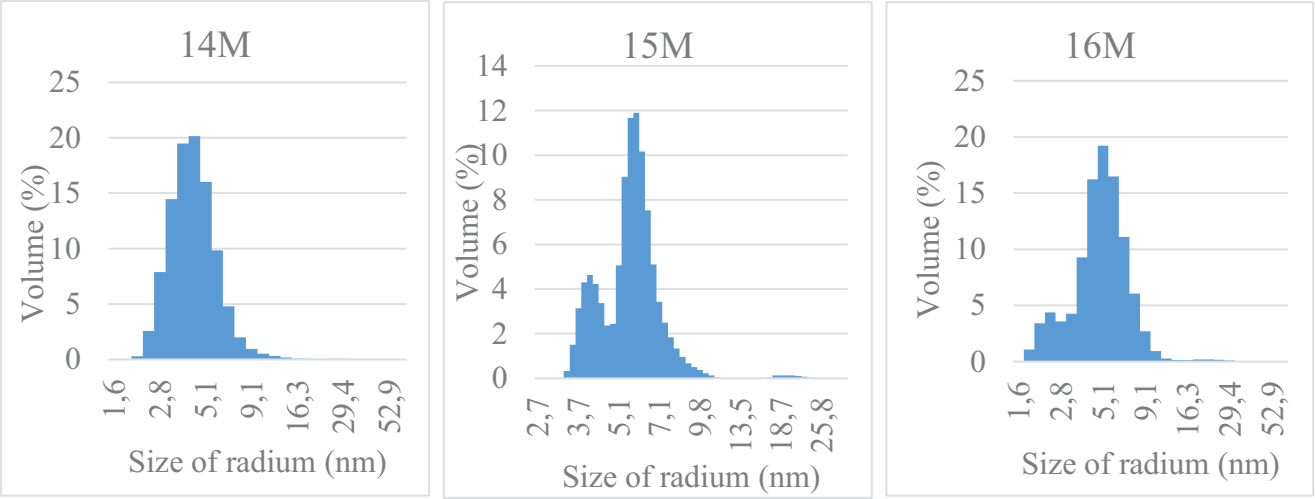

Fig. 5. Particle size distribution of *A. pernyi* fibroin in the solutions dissolved by different concentration of LiSCN.

4. Conclusions

The preparation process of *A. pernyi* fibroin aqueous solution was studied. By examination of each steps to make the aqueous solution from cocoons, the dialysis process was key step in the process to prepare the aqueous solution with stability and reproducibility and without gelation. A shorter dialysis time and a supplement of $CaCl_2$ in the dialysis solution at the first stage of dialysis was shown to make a better stability for the aqueous solution, and we established the proper process conditions for preparation of *A. pernyi* fibroin aqueous solution. The first stage of dialysis includes 25 mM of $CaCl_2$ and is performed for 150 minutes in order to stably remove the lithium thiocyanate from the fibroin solution. The second stage is similar but for only 1 h. It is purposely to make sure that no remaining lithium thiocyanate is present in the solution. The four following stages of the dialysis are 1 h each with pure water to remove the excess of $CaCl_2$. The total length time of the dialysis is calculated at 7.5 hours.

5. References

1) X.-Y. Luan, G.-H. Huo, M.-Z. Li, S.-Z. Lu and X.-G. Zhang (2009): *Antheraea pernyi* silk fibroin maintains the immunosupressive properties of human bone marrow mesenchymal stem cells, Cell Biol Int., **33**, 1127–1134.

2) Y. Liu, R. You, G. Liu, X. Li, W. Sheng, J. Yang and M. Li (2014): *Antheraea pernyi* silk fibroin-coated pei/dna complexes for targeted gene delivery in hek 293 and hct 116 cells, Int J Mol Sci, **15**, 7049–7063.

3) C. Ma, L. Lv, Y. Liu, Y. Yu, R. You, J. Yang and M. Li (2014): *Antheraea pernyi* silk fibroin for targeted gene delivery of vegf165-ang-1 with pei, Biomed Mater, **9**, 035015.

4) Q. Fang, D. Chen, Z. Yang and M. Li (2009): In vitro and in vivo research on using *Antheraea pernyi* silk fibroin as tissue engineering tendon scaffolds, Mater Sci Eng, C, **29**, 1527–1534.

5) J. Wang, B. Sun, M. A. Bhutto, T. Zhu, K. Yu, J. Bao, Y. Morsi, H. El-Hamshary, M. El-Newehy and X. Mo (2017): Fabrication and characterization of *Antheraea pernyi* silk fibroin-blended p (lla-cl) nanofibrous scaffolds for peripheral nerve tissue engineering, Front Mater Sci, **11**, 22–32.

6) H. Sezutsu and K. Yukuhiro (2000): Dynamic rearrangement within the *Antheraea pernyi* silk fibroin gene is associated with four types of repetitive units, J Mol Evol, **51**, 329–338.

7) N. Minoura, S.-I. Aiba, M. Higuchi, Y. Gotoh, M. Tsukada and Y. Imai (1995): Attachment and growth of fibroblast cells on silk fibroin, Biochem Biophys Res Commun, **208**, 511–516.

8) A. Varone, D. Knight, S. Lesage, F. Vollrath, A. Rajnicek and W. Huang (2017): The potential of *Antheraea pernyi* silk for spinal cord repair, Sci Rep-Uk, **7**, 13790.

9) M.-K. Kim, K.-Y. Yoo, K.-J. Kwon, S.-G. Kim, Y.- W. Park, K.-G. Lee, Y.-Y. Jo and H.-Y. Kweon (2014): Powdered wound dressing materials made from wild silkworm *Antheraea pernyi* silk fibroin on full-skin thickness burn wounds on rats, Maxillofac Plast Reconstr Surg, **36**, 111.

10) W. Tao, M. Li and C. Zhao (2007): Structure and properties of regenerated *Antheraea pernyi* silk fibroin in aqueous solution, Int J Biol Macromol, **40**, 472–478.

11) H. Wang, Y. Zhang, H. Shao and X. Hu (2005): A study on the flow stability of regenerated silk fibroin aqueous solution, Int J Biol Macromol, **36**, 66–70.

12) H. Kweon and Y. H. Park (2001): Dissolution and characterization of regenerated *Antheraea pernyi* silk fibroin, J Appl Polym Sci, **82**, 750–758.

13) S. Yan, C. Zhao, X. Wu, Q. Zhang and M. Li (2010): Gelation behavior of *Antheraea pernyi* silk fibroin, Sci China Chem, **53**, 535–541.

14) J. Kaur, R. Rajkhowa, T. Tsuzuki and X. Wang (2015): Crystals in *Antheraea assamensis* silkworm cocoon: Their removal, recovery and roles, Mater Design, **88**, 236–244.

15) T. Gheysens, A. Collins, S. Raina, F. Vollrath and D. P. Knight (2011): Demineralization enables reeling of wild silkmoth cocoons, Biomacromolecules, **12**, 2257–2266.

16) J. Guan, W. Zhu, B. Liu, K. Yang, F. Vollrath and J. Xu (2017): Comparing the microstructure and mechanical properties of *Bombyx mori* and *Antheraea pernyi* cocoon composites, Acta biomater, **47**, 60–70.

17) S. Du, J. Li, J. Zhang and X. Wang (2015): Microstructure and mechanical properties of silk from different components of the *Antheraea pernyi* cocoon, Mater Design (1980-2015), **65**, 766–771.

18) B. Zuo, L. Liu and F. Zhang (2009): Structure and properties of regenerated *Antheraea pernyi* silk fibroin filaments, J Appl Polym Sci, **113**, 2160–2165.

Chapter 3: Characterization of *Antheraea pernyi* fibroin in the aqueous solution prepared by new process

Chapter 3: Characterization of the aqueous solution of *A. pernyi* prepared by an improved process.

1. Introduction

As shown in chapter 2, we succeeded to develop the new process for preparation of *A. pernyi* fibroin aqueous solution with stability and reproducibility. In this chapter, characterization of the *A. pernyi* fibroin prepared by the new process was performed. In the process, since $CaCl_2$ was used during the dialysis step, the resulting *A. pernyi* fibroin molecules may be different in properties from *A. pernyi* fibroin of the other reported preparation methods. The molecular weight and the distribution of our *A. pernyi* fibroin were determined and compared with those of the reported results in previous literatures. And we measured Ca^{2+} concentration in the aqueous solution and calculated the Ca^{2+} amount incorporated in the *A. pernyi* fibroin molecules, because we inferred the Ca^{2+} ions may play an important role on the stability of *A. pernyi* molecules in the aqueous solution. Further we examined the gelation ability of the *A. pernyi* fibroin from the aqueous solution. The gelation ability is very important for fabricating the *A. pernyi* fibroin to materials with various forms based on water solvent process. If we can control the gelation behavior, it will make possible to manage the fabrication process for production of *A. pernyi* fibroin materials.

2. Materials and Methods

2.1 *A. pernyi* cocoons

We obtained the cocoons of *A. pernyi* silkworms from the farm in Shinshu University.

2.2 Preparation of silk fibroin solution

A. pernyi cocoons were cut in small pieces and degummed three times at 95 to 98 °C in a 2.5 w/v% Na_2CO_3 solution for 30 mins. After each degumming process, the fibers were washed three times with hot water and dried at 50 °C overnight. The degummed fibers were then dissolved in 15 M lithium thiocyanate (LiSCN, Wako pure chemical Co. Ltd., Japan) at 45 °C for 1h and dialysed for 7.5 hours in 25 mM $CaCl_2$ and water with 6 changes of dialysate in a cellulose dialysis tube (MWCO 6000-8000, Spectrapore, Tokyo, Japan). The resulting fibroin solution was stored at 4 °C prior use.

2.3 Analytical methods

The molecular weight of the *A. pernyi* fibroin in the aqueous solution was estimated by SDS-PAGE using PAGEL (5- 20% gradient gel, ATTO Co. Ltd., Tokyo, Japan) and electrophoresis buffer added 2 M Urea. Molecular weight standard was used (ZE-Protein Standard, WSE-7020, ATTO Co. Ltd., Tokyo, Japan).

2.4 Gelation

For evaluating the gelation time of the aqueous solution, 2 mL of the 1 and 5 wt% solutions were put into a microtube and incubated at 4, 25, 37, and 50 ℃. The gelation time was defined as the time when the fibroin solution does not flow out from the microtube by placing the tube upside down.

3. Results and discussion

3.1 Molecular weight of the fibroin in the aqueous solution

To determine the molecular weight and the distribution of *A. pernyi* fibroin prepared by our process, SDS-PAGE was performed. It was difficult to proceed SDS-PAGE of *A. pernyi* fibroin by typical protocol because gelation was occurring during electrophoresis. For preventing the gelation, we used the buffer adding 2 M Urea. Figure 1 shows the result of the SDS-PAGE. Clear bands were observed at around 23 kDa, and 8 kDa, and smear band between 5 kDa and 200 kDa continuously was presented. The estimated Mw of *A. pernyi* by calculating the gene sequence is 216 kDa [1]. This result indicates that *A. pernyi* fibroin in our aqueous solution was degraded during the preparation process. However, the SDS-PAGE pattern is similar with the result reported by Tao et al. [2] that explained the main degradation of the silk fibroin comes from the destruction and dissolution of a portion of covalent bonds and secondary bonds.

Therefore, by comparison, the molecular degradation was caused by degumming and dissolving *A. pernyi* fiber with LiSCN, not due to our dialysis process. Recovery rate of *A. pernyi* fibroin was 50.5 ±4.0 % (N =10) which was calculated from the final concentration of *A. pernyi* fibroin aqueous solutions by the amount of the degummed *A. pernyi* fibroin fibers at dissolving. We infer the high molecular weight of *A. pernyi* fibroin molecules are cleaved by degumming and dissolving treatment and removed during dialysis process.

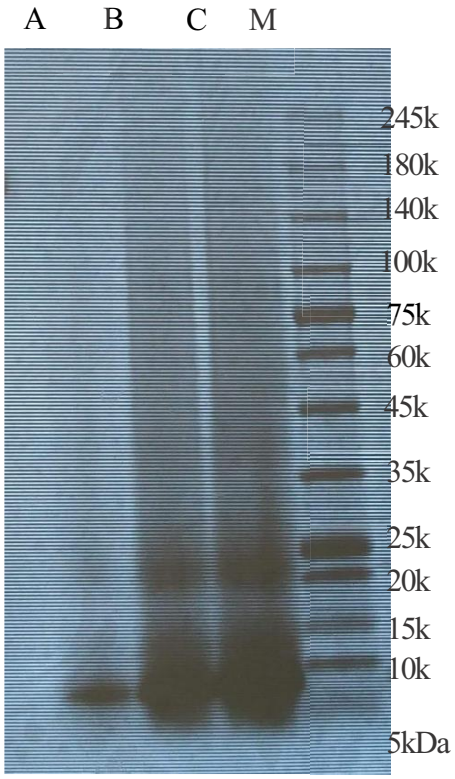

Fig. *1.* SDS-PAGE results of *A. pernyi* fibroin in aqueous solution prepared by our dialysis process. Lanes A, B and C present the *A. pernyi* fibroin samples applied at 2 μL, 4μL and 6μL respectively. Lane M indicates the molecular weight marker.

3.2 Gelation of *A. pernyi* aqueous solution

Gelation ability of the *A. pernyi* aqueous solution is important to make *A. pernyi* materials such as film, sponge, and nanofiber by self-assembly process. The gelation times of the *A. pernyi* aqueous solution prepared by our improved dialysis process at 5 and 1 wt% concentrations were evaluated at 4, 25, 37, and 50 ℃, and the results were summarized in Table 1. No gelation was observed in 4 ℃ condition for more than two months. This result indicates that our *A. pernyi* aqueous solution is stable without gelation in a refrigerator. The gelation time became shorter with the increase of temperature and of the concentration. Yan et al., reported the gelation behaviour of *A. pernyi* aqueous solution prepared by dissolving with melted $Ca(NO_3)_2$ followed the typical dialysis process against water, and presented decreasing the gelation time by increasing temperature and concentration [3]. The results shown in Table 3 are similar with them. They also reported the influence of Ca^{2+} on gelation and presented that addition of 5 mM Ca^{2+} led to the decrease of the gelation time but more than 10mM Ca^{2+} resulted in prolonging the gelation time. As mentioned above, our *A. pernyi* fibroin molecules incorporated with 260 ppm of Ca^{2+} ion during the dialysis process and the amount of Ca^{2+} are comparable with the 6.5 mM concentration. Therefore, while Ca^{2+} ions incorporated in molecules will prevent self-aggregation at low temperature as mentioned above, the molecular mobility will become more active at higher temperature and will increase the opportunity for the PAB domains to have inter and intra contact and will result in molecular aggregation by overcoming the Ca^{2+} repulsive effect. This

result indicates our *A. pernyi* aqueous solution can be fabricated into water insoluble materials by temperature control.

Table 1. Gelation time of *A. pernyi* aqueous solutions at different temperatures. *: No gelation for more than 2 months

T°C	5wt% Time (min)	10wt% Time (min)
4	-*	-*
25	240	300
37	45	30
50	5	5

3.3 Role of $CaCl_2$ for delaying gelation

The addition of $CaCl_2$ to the dialysis solution at the beginning process was effective for the preparation of *A. pernyi* aqueous solution with stability and reproducibility. To investigate the role of $CaCl_2$, the amount of Ca^{2+} ions in the *A. pernyi* aqueous solution was determined by ICP measurement. 260 ppm of Ca^{2+} ion existed in the solution. 25 mM $CaCl_2$ was used in the dialysis solution and the dialysis solution was changed to pure water by a change total of four times. The volume ratio of *A. pernyi* solution and dialysis solution was 1:150 for each time. Based on these conditions, the theoretical amount of Ca^{2+} ions which should be presented in the *A. pernyi* aqueous solution, can calculate to be 5.47×10^{-5} ppm. This result indicates the amount of Ca^{2+} ions that was

existing into the *A. pernyi* molecules. The amino acid sequence of *A. pernyi* is expected to consist repeating motifs, which is the tandemly joined domains containing the polyalanine block (PAB) and the nonpolyalanine block (NPAB) [4]. PAB domains have a hydrophobic nature and tend to make self-aggregates through hydrophobic interactions in water, and NPAB shows relatively hydrophilic nature and present many acidic amino acids like aspartic acid. Ca^{2+} ions can bind to the acidic amino acid residues in the NPAB through ionic interaction and will make *A. pernyi* molecules a high charge density. An electrical repulsive force by the additional charge at NPAB may prevent the self-aggregation at PAB resulting among the *A. pernyi* molecules in water.

4. Conclusions

Characteristics of *A. pernyi* fibroin in the aqueous solution prepared by our new process were determined. Decrease of molecular weight and the molecular weight distributions were observed on our *A. pernyi* fibroin, but the results were similar with those of *A. pernyi* fibroin reported in pervious literatures. We found Ca^{2+} molecules incorporated in our *A. pernyi* fibroin at 260 ppm concentration. The gelation of the *A. pernyi* fibroin aqueous solution occurred by raising the temperature. This result indicates that our *A. pernyi* fibroin aqueous solution can be used for fabrication of *A. pernyi* fibroin materials.

5. References

1) H. Sezutsu and K. Yukuhiro (2000): Dynamic rearrangement within the *antheraea pernyi* silk fibroin gene is associated with four types of repetitive units, J Mol Evol, **51** (4), 329–338.

2) W. Tao, M. Li, and C. Zhao (2007): Structure and properties of regenerated *antheraea pernyi* silk fibroin in aqueous solution, Int J B Macromol, **40** (5), 472–478.

3) S. Yan, C. Zhao, X. Wu, Q. Zhang, and M. Li (2010): Gelation behavior of *antheraea pernyi* silk fibroin, Sci China Chem, **53** (3), 535–541.

4) H. Sezutsu and K. Yukuhiro (2000): Dynamic rearrangement within the Antheraea pernyi silk fibroin gene is associated with four types of repetitive units, J Mol Evol, 51, 329–338.

Chapter 4: Characterization of *Antheraea pernyi* fibroin films from the aqueous solution prepared by an improved process.

Chapter 4: Characterization of *Antheraea pernyi* fibroin films from the aqueous solution prepared by an improved process.

1. Introduction

Wild silks are studied since many years to aim at the development of medical materials, especially cells scaffold for tissue engineering in regenerative medicine. The normal silk, *Bombyx mori* (B.*mori*), is the most used nowadays because of its strong biocompatibility with cells and its easy processing [1, 2]. The *B. mori* is non-toxic and allows mammal cells to adhere and proliferate. Already used as suture [3], it keeps giving new possibilities for clinical treatments and is used as biomedical materials such as controlled drug release carriers or repair materials for bones, ligament and so on. In comparison, wild silks such as *Antheraea pernyi* offer the same properties but thanks to its Arg-Gly-Asp (RGD) tripeptide sequence [4] in its molecule, its fibroin offers an enhancement of cell adhesion and proliferation. This sequence can bind to integrin receptors in cell membrane and facilitate adhesion of cells [1, 5 - 6]. Reports have shown its ability to support human bone marrow derived mesenchymal stem cells [7] and fibroblast cells [8].

As described in chapter 2, we can prepare *A. pernyi* fibroin aqueous solution with stability and reproducibility, and in chapter 3, the gelation ability of the *A. pernyi* fibroin aqueous solution was confirmed. The result indicates that the fabrications of *A. pernyi* fibroin from the aqueous solution to various forms can be facilitated by our new process.

In this chapter, the properties of the *A. pernyi* fibroin materials fabricated from the process were evaluated for seeking the possibilities of applications of the materials. We especially focused on the surface properties of our *A. pernyi* fibroin film coated on substrate aimed to be used as a biomaterial for cell scaffold in tissue engineering. Surface morphology was observed by AFM and the physicochemical properties were determined by contact angle and zeta potential measurements. Cell compatibility was evaluated by cell adhesion and proliferation test, and cell mobility was determined by time laps experiment. The results obtained in our *A. pernyi* fibroin film from the aqueous solution prepared by our new process were compared with the results in the published papers when possible.

2. Materials and Methods

2.1 Preparation of *A. pernyi* fibroin aqueous solution

A. pernyi silkworms were bred at the farm of Shinshu University, Ueda, and the collected and stored cocoons were supplied. The cocoons were cut in small pieces and degummed with 2.5 w/v% Na_2CO_3 solution at 95-98 °C for 30 min, and then washed three times with hot water and dried at 50 °C overnight. This process was repeated three times. The then degummed fibers were dissolved in 15 M lithium thiocyanate (LiSCN, Wako pure chemical Co. Ltd., Japan) at 45 °C for 1h in a water bath. They were then dialyzed following the previously reported process [10].

B. mori fibroin was prepared by degumming one time in 0.02 M $NaHCO_3$ solution at 95-98 °C for 30 min and washed three times with 90 °C pure water and air dried overnight. The fibers were then dissolved in 9.0 M LiBr and dialysis against pure water for three days.

The concentration of the aqueous solutions was determined by weighting the remaining solid after drying the solution.

2.2 Coating

2.2.1 Surface analysis.

The *A. pernyi* fibroin aqueous solution was coated on glass disks (Ø 15 mm, Matsunami co. Ltd., Tokyo, Japan) for contact angle, zeta-potential, AFM, and FT-IR measurements. Coating was performed by dipping the aqueous solution at a concentration of 10 mg/mL for 30 minutes and drying overnight at room temperature. To evaluate the effect of methanol treatment, the coated glass disks were immersed in 80% methanol solution for 30 minutes and dried at room temperature to prevent the formation of gel due to the low temperature stability of the solution [10].

2.2.2 Cell culture.

1 w/v% of *A. pernyi* fibroin aqueous solution was coated on the surface of the culture plate (24 wells culture dish, TPP AG, Switzerland) for 30 minutes. Then the solution was removed, and the coated plates were dried overnight at 4 °C to prevent a complete gelation of the aqueous solution. The coated *A. pernyi* fibroin was insolubilized by 80% methanol treatment and sterilized by 70% ethanol before cell culture test.

2.3 Analytical methods

The structures of the coated *A. pernyi* fibroin were examined by Fourier Transform Infrared Spectrometer with Attenuated Total Reflection apparatus (ATR-FTIR, IRT-Tracer-100, Shimadzu, JAPAN), and the surface morphology was observed by Scanning Probe Micrograph (SFT-3500, Shimadzu, JAPAN). The hydrophobicity of the coated

surface was measured by contact angle (VCA Optima-XE, AST-products, USA). The contact angles were taken by 30 FPS video recording and determined by extrapolation to zero time from the data. The zeta potential of the coated *A. pernyi* fibroin was taken by an Electrophoretic Light Scattering Spectrophotometer (Photal LEZA-600, Otsuka, JAPAN) at pH 3 to 9.

2.4 Cell NIH3T3

NIH3T3 cells used for cell culture test were obtained from Riken Bioresource Center (ID: RCB1862, Riken Bioresource Center, Tsukuba, Japan).

Cell adhesion test on the coated *A. pernyi* fibroin was performed as follows. 50 000 cells/mL/well were seeded on each sample and incubated for 3 hours at 37 °C and 5 % CO_2. After incubation, each well was rinsed by PBS for removing non-adhered cells and then 0.5% Triton X-100/PBS solution was added for cell number counting by LDH activity measurement.

Cell proliferation test on the coated *A. pernyi* fibroin was performed as follows. 5,000 cells/mL /well were seeded on each sample and incubated at 37 °C and 5 % CO_2. After 1, 3, 5, and 7 days of incubation, PBS rinsing and addition of Triton X-100/PBS were performed as same as cell adhesion test described above for cell number counting on each culture day.

The number of cells was determined by LDH activity measurement method [11]. Briefly, the LDH activity from cell lysate in Triton-X 100/PBS solution was measured

by NADH consumption using the change of the optical density at 340 nm. The cell number was calculated by calibration data using LDH activity against the known cell number.

Cell mobility on the coated *A. pernyi* fibroin was measured by time laps observation at the initial culture. Cells were seeded on a glass bottom dish (35mm Ø, Greiner, Germany) and cultured at 37 °C and 5 % CO_2. During culture, photos were taken on every 5 min till 15 hours. The cell mileage and speed were calculated using M-TrackJ and Image J frame per frame of the obtained video.

3. Results and Discussion

3.1 Structure of *A. pernyi* fibroin film

Fig shows Amide I and Amide II regions in the spectrum of *A. pernyi* fibroin coating films on glass disks with and without methanol treatment. From the FTIR measurement, no differences between our *A pernyi* fibroin film before methanol treatment and the other films reported previously were observed. A study reported by Zuo et al. showed the spectral pattern of the regenerated *A. pernyi* fibers prepared with LiSCN, and peaks at 1654 and 1541 cm^{-1}, attributed to the α-helix conformation, along with a band at 1515 cm^{-1} for the ß-sheet conformation were presented [12]. Li et al. showed a FTIR spectra of prepared regenerated film of *A. pernyi* prepared with LiSCN. Its graph showed peaks at 1655 and 1543 cm^{-1} for the α-helix conformation [13]. In

Figure 1, the peak at 1650 cm^{-1} attributed as α-helix and random coil in the spectrum of without methanol treatment was shifted to 1625 cm^{-1} as ß-sheet conformation after methanol treatment. The peak shift by methanol treatment is typical result for *B. mori* and *A. pernyi* fibroin [13 - 16]. Therefore, the secondary structure of our *A. pernyi* fibroin film are similar with that of *A. pernyi* fibroin materials prepared by typical dialysis process in reported studies [17].

Several Ca^{2+} ions were incorporated into our *A. pernyi* fibroin molecules during the new dialysis process as reported in our previous paper [10], and the amount was determined at 260 ppm. The number of Ca^{2+} ions incorporated in one *A. pernyi* fibroin molecule are calculated and are estimated to be less than 10. So, we infer the Ca^{2+} ions are binding in non-crystal regions containing acidic amino acids, not in crystal regions by poly-Ala sequence which are main regions to determine the secondary structures. Therefore, this result may also indicate that Ca^{2+} incorporation into the molecules made no influence on the secondary structure of *A. pernyi* fibroin in the film.

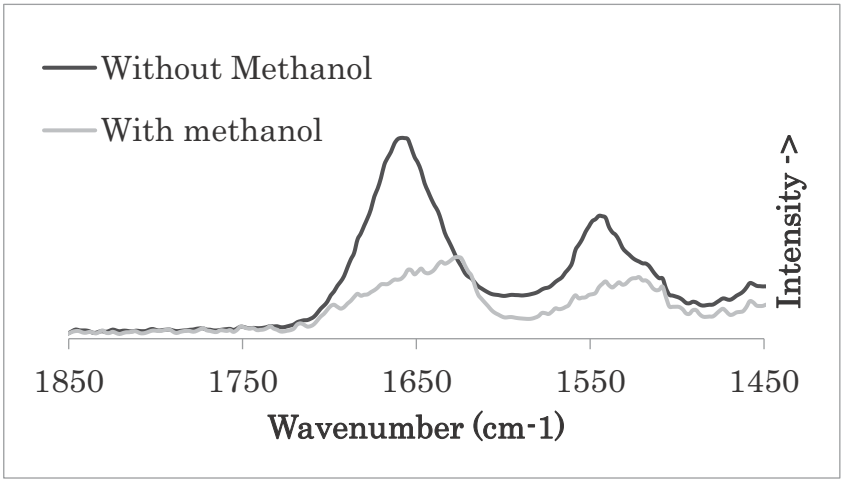

Fig 1. FTIR spectrum of *A. pernyi* fibroin coating film with/without methanol treatment.

3.2 Surface morphology of *A. pernyi* fibroin film

The morphology of our *A. pernyi* fibroin coating film on glass disk was observed by AFM measurement and the results are shown in Figure 2. Unfortunately, since we could not find any other results of AFM images concerning *A. pernyi* fibroin film in published literatures, the AFM image of *B. mori* fibroin coating film on glass disk was observed as the reference. As shown in Figure 2, the surface morphology of our *A. pernyi* fibroin film was different from that of *B. mori* fibroin film. Rougher shapes were observed on our *A. pernyi* fibroin film surface than on *B. mori*. The average height of the roughness is 18.07 nm ± 4.26 nm and 10.74 nm ± 2.44 nm, respectively. Mandel et al. [17] reported the AFM image of *Antheraea mylitta*, which is in the same family of wild silk with *Antheraea pernyi* and presented the similar globular morphology on the surface. The molecular interaction in fibroin of wild silks like *A. pernyi* and *A. mylitta* is stronger than that of *B. mori* fibroin. Wild silks fibroin molecules have the repeated poly-Ala sequences which are the main sequence to form crystal region by β-sheet conformation. In the case of B. mori fibroin molecule, the repeated crystal sequence is consisted of poly-(Ala-Gly). The binding energy of poly-Ala β-sheet is reported to be higher than that of poly-(Ala-Gly) β-sheet [18]. Therefore, we infer the self-aggregation process might occur more easily on wild silk fibroin during drying process to fabricate film than with B. mori fibroin. The resulting aggregations will construct the globular like roughness on *A. pernyi* fibroin film surface.

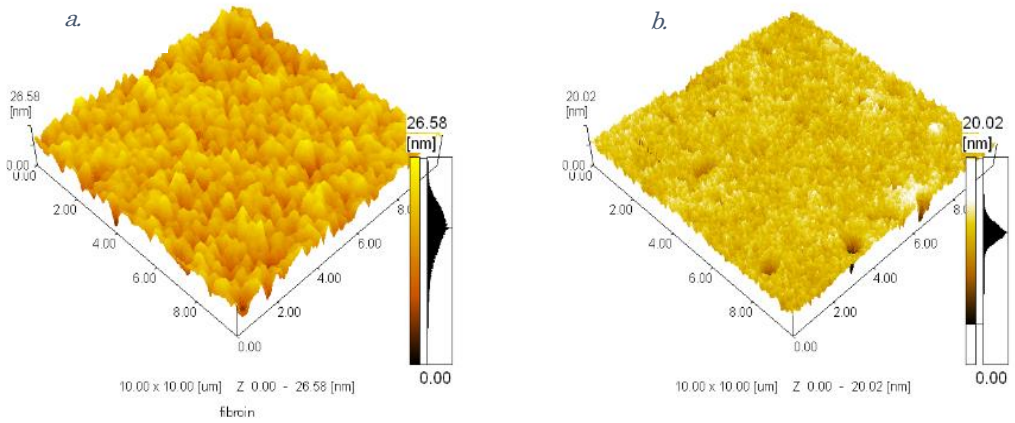

Fig 2. AFM images of a. *A. pernyi* fibroin film and b. *B. mori* fibroin coating film surface in the area of 10 μm²

3.3 Contact angle of *A. pernyi* fibroin film

Surface free energy and surface potential of the substrate are important physicochemical properties on interfacial events of the substrates like cell adhesion [19] and cell proliferation [11]. Contact angle measurement of our *A. pernyi* fibroin film was performed using water and diiodomethane, and the surface free energy was calculated from the contact angle data. The results are summarized in Table 1. For the calculation of the surface tension of *A. pernyi* film γ_s, we used following equation of Owens-Wendt [20] with the surface tension of water and diiodomethane that assumes that the normal surface tension is the sum of its polar and dispersive parts. Therefore, we used the constants: γ_L = 72.6, γ_L^d= 21.6 , γ_L^p= 51, and γ_L = 50.8, γ_L^d=48.5, γ_L^p=2.3 mN/m, for the

water and diiodomethane respectively. From the following equation, γ_S^d and γ_S^p are deducted from the double equation and added to obtain γ_s.

Equation: $\gamma_L(1+\cos(\theta)) = 2\sqrt{\gamma_L^d \gamma_S^d} + 2\sqrt{\gamma_L^p \gamma_S^p}$

The reported water contact angle of *A. pernyi* film are 62.4° ± 1.0° [21]. The result of our *A. pernyi* film indicates a slightly more hydrophilic surface compared with the reported *A. pernyi* film. We deduce the difference in water contact angle might come from the Ca^{2+} ions incorporated in *A. pernyi* fibroin during the preparation of our new dialysis process, because a hydration of Ca^{2+} could occur on the film surface. The surface tension (γ_s) of our *A. pernyi* fibroin film was calculated to be 56.2 mN/m (γ_S^d and γ_S^p are 42.2 and 14.0 mN/m, respectively). No data about surface tension of other *A. pernyi* films were published within our database research, but the surface energy of *B. mori* fibroin film from the aqueous solution was reported in 42 mJ/m^2 [22].

Table 1. Physicochemical properties of *A. pernyi* coating film surface.

Water contact angle (°)	Diiodomethane contact angle	Surface tension (mN/m)
55.4 ± 2.6	62.4 ± 1.0	56.2

3.4 Zeta potential of *A. pernyi* fibroin film

Figure 3 shows the pH dependence of the zeta-potential on the surface of our *A. pernyi* coating films on glass with the zeta-potential of the glass. The zeta-potential of our *A. pernyi* fibroin was 17.10 ± 0.30 mV, 15.93 ± 1.76 mV, -22.52 ± 4.75 mV and -27.39 ± 1.00 mV for pH 3, 5, 7 and 9 respectively. Unfortunately, we couldn't find any reported papers about zeta potential on *A. pernyi* silk fibroin to be compared with our data. The zeta potential of *B. mori* fibroin film was reported and the data at pH 7 was of the range from -24.41 to -31.5 mV [23]. The isoelectric point of both *A. pernyi* and *B. mori* fibroin is close to 4.5 [24, 25]. Therefore, the electric property of these fibroin surfaces was expected to be similar for their zeta-potential measurements. Thus, the zeta-potential of *A. pernyi* fibroin films was assumed at the similar value with *B. mori* fibroin film. However, the zeta-potential of our *A. pernyi* fibroin film is a negatively lower than that of *B. mori* fibroin.

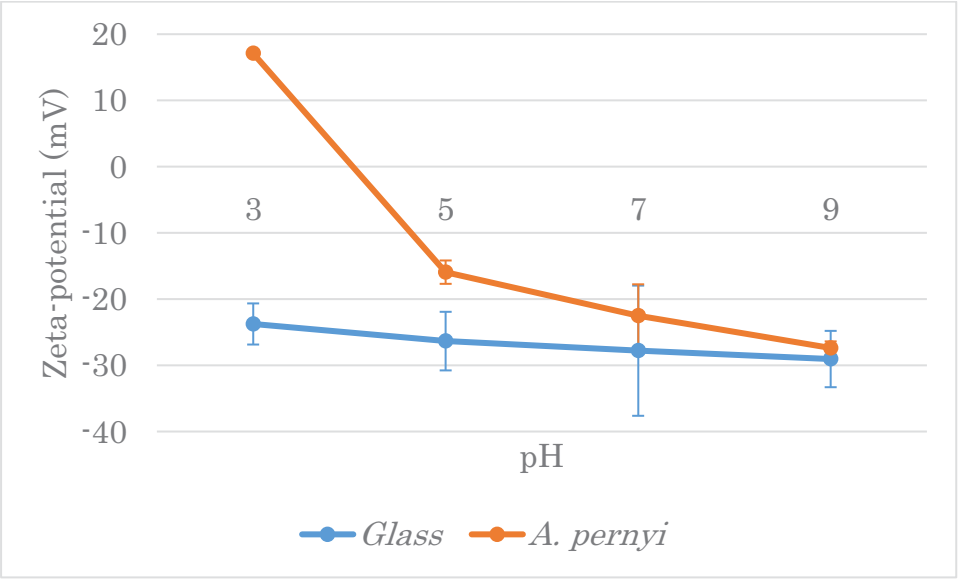

Figure 3. Zeta-potential on the surface of glass and *A. pernyi* fibroin coating film (N=3)

3.5 Cell culture

3.5.1 Cell adhesion and proliferation on *A. pernyi* film

To evaluate cell compatibility of our *A. pernyi* fibroin, cell adhesion and proliferation test were performed on the coating films. The results of NIH3T3 cell adhesion are presented in Figure 4. As shown in Figure 4, the number of adhered cells on *A pernyi* film was significantly higher than *B. mori* fibroin and TCPS as control. Figure 5 presented the cell shapes after 280 minutes of cell culture on *A. pernyi* and *B. mori* fibroin coating film. Clear difference on cell morphology between two substrates were observed at this early stage of culture. Cells on the *A. pernyi* fibroin substrate showed spreading shape comparing with cells on B. mori fibroin substrate which showed round morphologies. This result indicates that cell can adhere on the *A. pernyi* fibroin preferable than on *B. mori* fibroin. So, it was confirmed that the RGDS sequence in our A. pernyi fibroin can work well to support cell adhesion. Good cell adhesion on *A. pernyi* film have been reported in previous papers [7] thanks to the RGDS sequence in the molecule [4]. In the case of our *A. pernyi* fibroin film prepared by the new process, cell adhesion property can keep a good adhesion property even by changing the surface physicochemical properties as mentioned above. Figure 6 presents the result of cell proliferation test. Cells could proliferate on our *A. pernyi* fibroin film like on *B. mori* fibroin and TCPS. The shape of cells proliferated from day 1 to day 5 on the substrates

are shown in Figure 7. No obvious differences about the cell shapes were observed among *A. pernyi*, *B. mori*, and TCPS. These results indicate cells can proliferate normally on our *A. pernyi* fibroin substrate. Our *A. pernyi* fibroin film can promote cell adhesion and can support cell proliferation as efficiently as *B. mori* fibroin and TCPS.

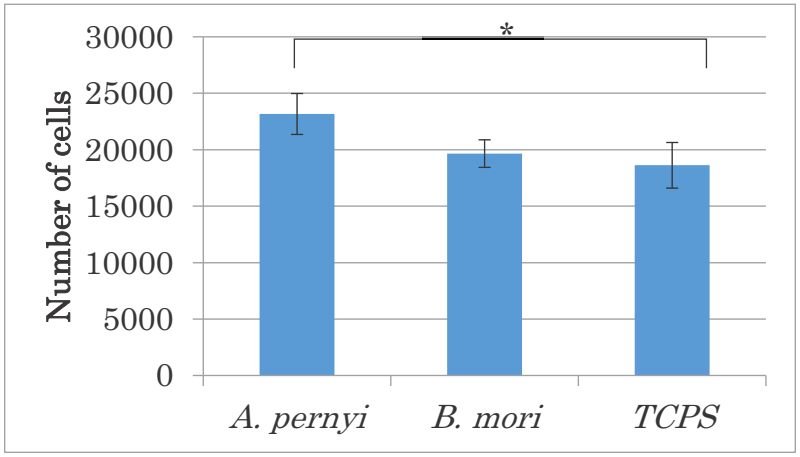

Fig 4. Cell Adhesion on *A. pernyi* and *B. mori* fibroin coating film. * significant difference ($p<0.05$)

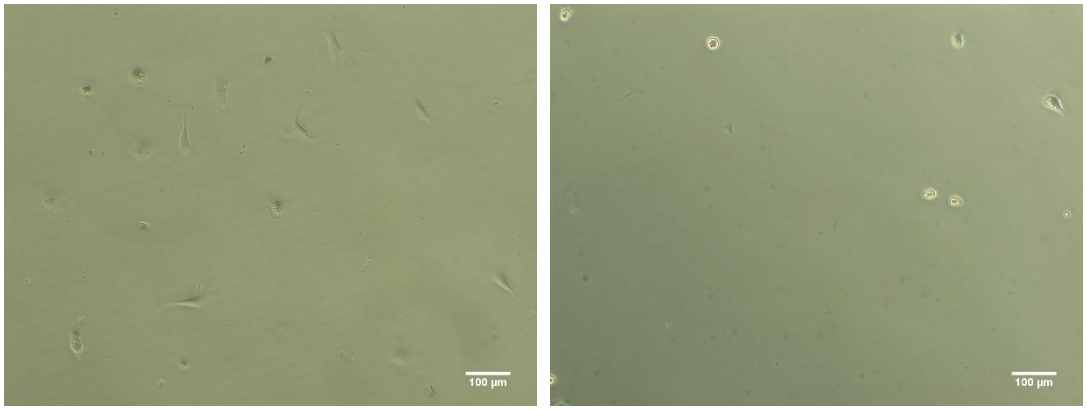

Fig 5. Comparison of cell morphology after 280 minutes of cell culture on *A. pernyi* (left) and *B. mori* (right) fibroin coating films.

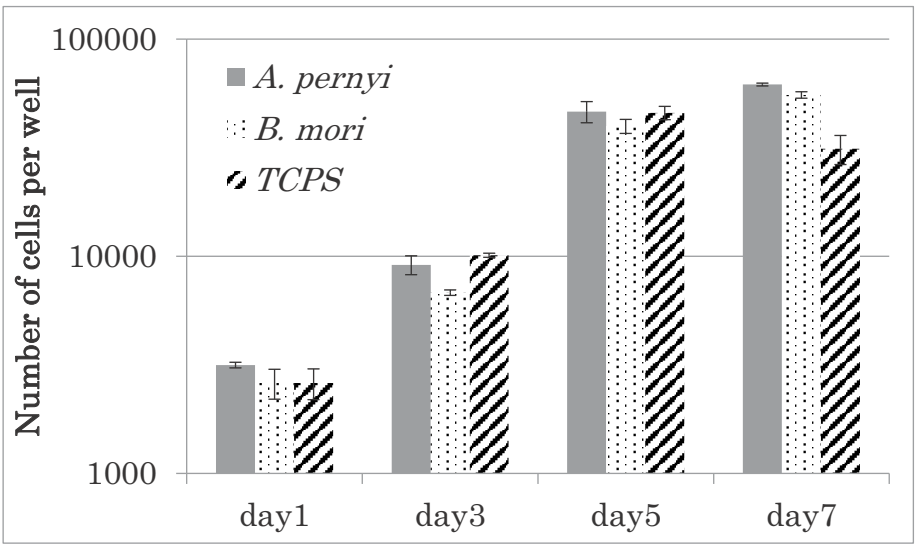

Fig 6. Cell proliferation on *A. pernyi* and *B. mori* fibroin coating film.

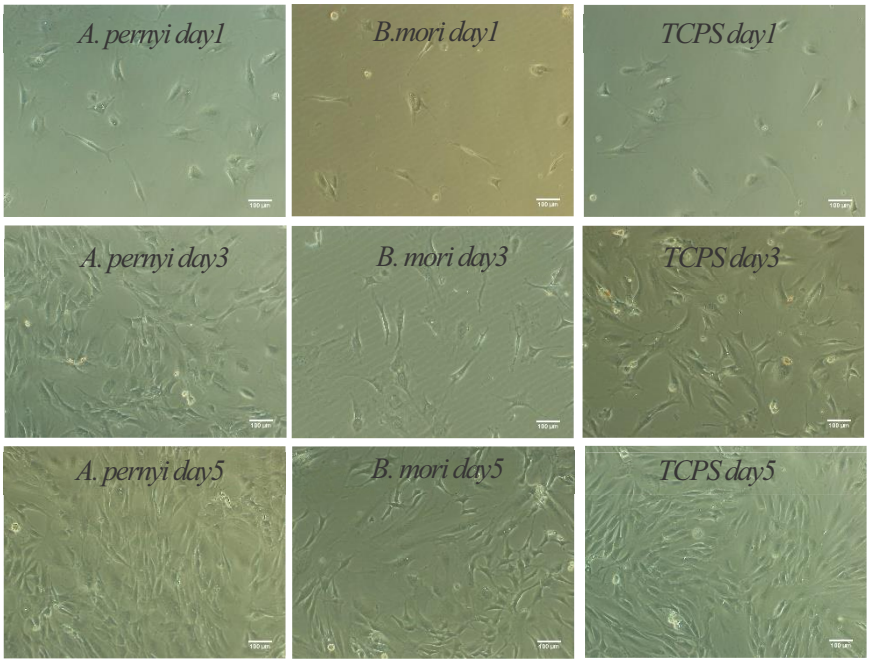

Fig 7. Cell morphology on *A. pernyi* and *B. mori* fibroin coating films during cell proliferation

3.5.2 Cell mobility

Cell mobility will be one of the interesting phenomena of cell behavior. We reported highly active cell mobility on *B. mori* fibroin substrate and the high gene expression related with extracellular matrix corresponding to the high cell mobility [26]. The cell mobility on *A. pernyi* and *B. mori* fibroin substrate at the initial stage of the culture were determined and the results are summarized in Table 2. Higher cell mobility on *B. mori* substrate was observed as reported previously. On the contrary, cell mobility on *A. pernyi* substrate decreased to approximately half of that on *B. mori* substrate. Probably the RGDS sequence in *A. pernyi* fibroin molecules may work to inhibit cell moving through the cell adhesion function. The result indicates that a different function on cell behaviors from *B. mori* fibroin can be expected to be provided by our *A. pernyi* fibroin for developing a new biomaterial.

Table 2: Average mileage and speed of cells cultured on *A. pernyi* and *B. mori* fibroin coating films.

	Mileage	Speed
A. pernyi	164.13 μm ± 49.99	0.187 μm/min ± 0.06
B. mori	282.58 μm ± 55.36	0.323 μm/min ± 0.07

4. Conclusions

Characterizations of *A. pernyi* fibroin coating films fabricated from the aqueous solution that was prepared by our new process was studied. The secondary structure of our *A. pernyi* fibroin was the same with the reported results by the other papers. The roughness of the surface was higher than that of *B. mori* fibroin film surface by AFM observation. More hydrophilic and lower zeta potential was observed on our *A. pernyi* fibroin film than on the reported *A. pernyi* fibroin film. These physicochemical properties are characteristic of our *A. pernyi* fibroin. Cell adhesion and proliferation on our *A. pernyi* fibroin film was as good as on *B. mori* fibroin film. However, cell mobility on our *A. pernyi* fibroin film was estimated at the half the speed of *B. mori* fibroin film. These results suggest our *A. pernyi* fibroin have a possibility to be used as a biomaterial with the different characters from *B. mori* fibroin and *A. pernyi* fibroin reported previously.

5. Acknowledgement

This study was partially supported by NIMS Joint Research Hub Program and by NIMS Molecule & Material Synthesis Platform in "Nanotechnology Platform Project" operated by the Ministry of Education, Culture, Sports, Science and Technology (MEXT), Japan.

6. References

1) N. Minoura, S.-I. Aiba, M. Higuchi, Y. Gotoh, M. Tsukada and Y. Imai (1995): Attachment and growth of fibroblast cells on silk fibroin, Biochem Bioph Res Co, **208** (2), 511–516.

2) Y. Gotoh, M. Tsukada and N. Minoura (1998): Effect of the chemical modification of the arginyl residue in *Bombyx mori* silk fibroin on the attachment and growth of fibroblast cells, J Biomed Mater Res: An Official Journal of The Society for Biomaterials, The Japanese Society for Biomaterials, and the Australian Society for Biomaterials, **39** (3), 351–357.

3) R. L. Moy, A. Lee and A. Zalka (1991): Commonly used suture materials in skin surgery, Am Fam Physician, **44** (6), 2123–2128.

4) H. Sezutsu and K. Yukuhiro (2000): Dynamic rearrangement within the *Antheraea pernyi* silk fibroin gene is associated with four types of repetitive units, J Mol Evol, **51** (4), 329–338.

5) M. D. Pierschbacher and E. Ruoslahti (1984): Cell attachment activity of fibronectin can be duplicated by small synthetic fragments of the molecule, Nature, **309** (5963), 30–33.

6) M. D. Pierschbacher and E. Ruoslahti (1984): Variants of the cell recognition site of fibronectin that retain attachment-promoting activity, P Natl Acad Sci Usa, **81** (19), 5985–5988.

7) X.-Y. Luan, Y. Wang, X. Duan, Q.-Y. Duan, M.- Z. Li, S.-Z. Lu, H.-X. Zhang, and X.-G. Zhang (2006): Attachment and growth of human bone marrow derived mesenchymal stem cells on regenerated *Antheraea pernyi* silk fibroin films, Biomed Mater, **1** (4), 181.

8) N. Minoura, S.-I. Aiba, Y. Gotoh, M. Tsukada, and Y. Imai (1995): Attachment and growth of cultured fibroblast cells on silk protein matrices, J Biomed Mater Res, **29** (10), 1215–1221.

9) W. Tao, M. Li, and C. Zhao (2007): Structure and properties of regenerated *Antheraea pernyi* silk fibroin in aqueous solution, Int J Biol Macromol, **40** (5), 472–478.

10) S. Rozet and Y. Tamada, (in press): An improved process for stably preparing of *Antheraea pernyi* fibroin aqueous solution, Nippon Silk Gakk, **27**.

11) Y. Tamada and Y. Ikada (1994): Fibroblast growth on polymer surfaces and biosynthesis of collagen, J Biomed Mater Res, **28** (7), 783–789.

12) M. Li, W. Tao, S. Lu, and S. Kuga (2003): Compliant film of regenerated *Antheraea pernyi* silk fibroin by chemical crosslinking, Int J Biol Macromol, **32** (35), 159–163.

13) P. Dubey, S. Murab, S. Karmakar, P. K. Chowdhury, and S. Ghosh (2015): Modulation of self-assembly process of fibroin: an insight for regulating the conformation of silk biomaterials, Biomacromolecules, **16** (12), 3936–3944.

14) X. Hu, D. Kaplan, and P. Cebe (2006): Determining beta-sheet crystallinity in fibrous proteins by thermal analysis and infrared spectroscopy, Macromolecules, **39** (18), 6161–6170.

15) X. Hu, D. Kaplan, and P. Cebe (2006): Determining beta-sheet crystallinity in fibrous proteins by thermal analysis and infrared spectroscopy, Macromolecules, 39 (18), 6161–6170.

16) X. Chen, Z. Shao, N. S. Marinkovic, L. M. Miller, P. Zhou, and M. R. Chance (2001): Conformation transition kinetics of regenerated Bombyx mori silk fibroin membrane monitored by time-resolved ftir spectroscopy, Biophys Chem, 89 (1), 25–34.

17) B. B. Mandal and S. C. Kundu (2008): Non-bioengineered silk gland fibroin protein: Characterization and evaluation of matrices for potential tissue engineering applications, Biotechnol Bioeng, **100** (6), 1237–1250.

18) C. Y. Hayashi, N.H. Shipley, and R. V. Lewis (1999): Hypotheses that correlate the sequence, structure, and mechanical properties of spider silk proteins, Int J Biol Macromol, 24 (2-3), 271-275.

19) Y. Tamada and Y. Ikada (1986): Cell attachment to various polymer surfaces, Polymers in medicine II, 101–115.

20) D. K. Owens and R. Wendt (1969): Estimation of the surface free energy of polymers, J Appl Polym Sci, **13** (8), 1741–1747.

21) L. J. Bray, S. Suzuki, D. G. Harkin, and T. V. Chirila (2013): Incorporation of exogenous rgd peptide and inter-species blending as strategies for enhancing human corneal limbal epithelial cell growth on *Bombyx mori* silk fibroin membranes, J Funct Biomater, **4** (2), 74–88.

22) O. N. Tretinnikov and Y. Tamada, (2001): Influence of casting temperature on the near-surface structure and wettability of cast silk fibroin films. Langmuir, **17** (23), 7406–7413.

23) D. Terada, Y. Yokoyama, S. Hattori, H. Kobayashi and Y. Tamada (2016): The outermost surface properties of silk fibroin films reflect ethanol-treatment conditions used in biomaterial preparation, Mater Sci Eng C, **58**, 119–126.

24) C.-Z. Zhou, F. Confalonieri, N. Medina, Y. Zivanovic, C. Esnault, T. Yang, M. Jacquet, J. Janin, M. Duguet and R. Perasso (2000): Fine organization of *Bombyx mori* fibroin heavy chain gene, Nucleic Acids Res, **28** (12), 2413–2419.

25) S. Yan, C. Zhao, X. Wu, Q. Zhang, and M. Li, (2010): Gelation behavior of *Antheraea pernyi* silk fibroin, Science China Chemistry, **53** (3), 535–541.

26) T. Hashimoto, K. Kojima, A. Otaka, Y. S. Takeda, N. Tomita and Y. Tamada (2013): Quantitative evaluation of fibroblast migration on a silk fibroin surface and TGFBI gene expression, J Biomater Sci Polym Ed, **24**, 158-169.

Chapter 5: Conclusions

Chapter 5: Conclusion

In this study, an improved preparation process for *A. pernyi* fibroin aqueous solution with stability and reproducibility was established successfully. This new process included a fine controlled dialysis step with addition of Ca^{2+} ions, which was found by carful examinations of each step in the preparation process. The aqueous solution was kept in liquid state without gelation for more than one month in the refrigerator. We inferred this stability of *A. pernyi* fibroin in aqueous solution might come from the Ca^{2+} ions incorporated with the molecules. The Ca^{2+} ions incorporation was found by ICP study. The aqueous solution could turn to gel by raising the temperature. This phenomenon is very important to fabricate *A. pernyi* fibroin to other materials. Thus, once the aqueous solution is prepared by the new process, the solution can store till further use in the refrigerator, and desired materials are manufactured by only raising temperature without any harmful regents. Actually, we demonstrated to fabricate the coating film using the *A. pernyi* aqueous solution in this study (in chapter 3). The secondary structure of *A. pernyi* fibroin in the film is the same as that of previously reported *A. pernyi* film. And the similar surface morphology of the film with *A. mylitta* fibroin film. These results indicate that the aqueous solution can be used for making *A. pernyi* coating material. Evaluation of cell culture on the coating film revealed no toxicity and good cell adhesion and proliferation. *A. pernyi* fibroin in the aqueous solution can be expected as a medical material like tissue engineering scaffold with biocompatibility.

This study gives great perspective for future application of this *A. pernyi* fibroin solution to be used in the medical field. There are still researches to do on the different scaffolds that are possible to make of this solution such as sponges or nanofibers.

Chapter 6: Accomplishments

1. Journal of publications

[1] S. Rozet and Y. Tamada, (in press): An improved process for stably preparing of *Antheraea pernyi* fibroin aqueous solution, Journal of Silk Science and Technology of Japan, 27 (in press).

[2] S. Rozet, H. Kobayashi, Z. Kajiura and Y. Tamada: Characterization of *Antheraea pernyi* fibroin films from the aqueous solution prepared by an improved process, Journal of Silk Science and Technology of Japan, Under review.

[3] Rebia, R. A., Rozet, S., Tamada, Y., & Tanaka, T. (2018): Biodegradable PHBH/PVA blend nanofibers: Fabrication, characterization, in vitro degradation, and in vitro biocompatibility. Polymer Degradation and Stability, 154, 124-136.

[4] Kharaghani, D., Khan, M., Shahzad, A., Inoue, Y., Yamamoto, T., Rozet, S., Tamada, Y., & Kim, I. (2018). Preparation and In-Vitro Assessment of Hierarchal Organized Antibacterial Breath Mask Based on Polyacrylonitrile/Silver (PAN/AgNPs) Nanofiber. Nanomaterials, 8 (7), 461.

[5] Ke MA, Sélène Rozet, Yasushi Tamada, Juming Yao and Qing-Qing Ni (2018), Multi-layer nanofibrous tubes with dual drug-release profiles for vascular graft engineering, Journal of Drug Delivery Science and Technology. Under revision.

2. Conferences

[1] Sélène Rozet, Mizuki Sasaki, Chisaki Watanabe, Zenta Kajiura and Yasushi Tamada, Cell behavior on *Bombyx Mori* silk fibroin mixed with *Antheraea pernyi* silk fibroin, The 24th International Congress on Sericulture and Silk Industry, Bangkok, Thailand, 2016.

[2] **Sélène Rozet**, Mizuki Sasaki, Chisaki Watanabe, Zenta Kajiura, and Yasushi Tamada, Cell behaviors on wild silks, *A. pernyi* and A. Yamamai, comparing with *Bombyx Mori* silk. The 9th International Silk Conference, China, 2016.

[3] **Sélène Rozet**, Ayano Kamiya and Yasushi Tamada, Preparation and characterization of *A. pernyi* fibroin aqueous solution, The Japanese Society of Silk Science and Technology, Tsukuba, Japan, 2017.

[4] **Sélène Rozet**, Ayano Kamiya, Yasushi Tamada and Zenta Kajiura, Preparation of wild silk (*A. pernyi*) fibroin aqueous solution and fabrication of wild silk materials, Advanced Material World Congress, Singapore, 2018.

[5] **Sélène Rozet,** Yasushi Tamada and Hisatoshi Kobayashi, Fabrication of *A. pernyi* fibroin materials from the aqueous solution, The Japanese Society of Silk Science and Technology, Kiryu, Japan, 2018.

3. Awards

[1] Outstanding Papers Competition, Cell behaviors on wild silks, *A. pernyi* and *A. yamamai* comparing with *Bombyx mori* silk, the 9th International Silk Conference, 2016, China.

[2] Best Oral Presentation Award, Preparation of wild silk fibroin aqueous solution for the fabrication of wild silk materials, Advancement Materials World Congress, 2018, Singapore

Chapter 7: Acknowledgements

Acknowledgment

Firstly, I would like to express my sincere gratitude to my advisor Prof. Y. Tamada for the continuous support of my Ph.D study and related research, for his patience, motivation, and immense knowledge. His guidance helped me in all the time of research and writing of this thesis. I could not have imagined having a better advisor and mentor for my Ph.D study.

Also, I would like to thank the rest of my thesis committee: Prof. Kobayashi from NIMS institution, who provided me an opportunity to have access to the laboratory and research facilities. Without this precious support it would not be possible to conduct this research. My sincere thanks also go Prof. Z. Kajiura for providing the base of this research and Prof. H. Moriwaki for being my tutor and helping me in cases of hardships.

Other thanks go to the Soroptimist group for their scholarship that made me able to pursue my study and gave me acknowledgement.

I thank my fellow lab mates in for the stimulating discussions, the teaching of Japanese and Japanese culture. Also, I thank my friend and former PhD student, Miss Peiffer thanks to whom I felt home in Japan and her guidance from her own experience.

Last but not the least, I would like to thank my family and my partner, for supporting me spiritually throughout writing this thesis and my life in general.